All Disordered Regions of Native Cellulose Show Common Low-Frequency Dynamics

Martin Müller,*,†,‡ Christoph Czihak,†,§,|| Helmut Schober,§ Yoshiharu Nishiyama,⊥ and Gero Vogl†,||

Institut für Materialphysik der Universität Wien, Strudlhofgasse 4, A-1090 Wien, Austria; European Synchrotron Radiation Facility, B. P. 220, F-38043 Grenoble Cedex, France; Institut Laue-Langevin, B. P. 156, F-38042 Grenoble Cedex 9, France; Hahn-Meitner-Institut, Glienicker Str. 100, D-14109 Berlin, Germany; and Graduate School of Agricultural and Life Sciences, The University of Tokyo, Yayoi, Tokyo 113-8657, Japan

Received July 26, 1999; Revised Manuscript Received December 13, 1999

ABSTRACT: We present inelastic neutron scattering (INS) experiments on various types of cellulose revealing the universal nature of the disordered regions from the point of view of low-energy dynamics. Using INS in combination with the deuteration of polar groups technique, we have studied the dynamic response of hydroxyl groups, χ'' within cellulose: $\chi''_{ac}(\omega)$ from regions accessible to water was found to be distinctly different from $\chi''_{inac}(\omega)$ obtained from the inaccessible crystal cores. The shape of $\chi''_{ac}(\omega)$ does not depend on the sample origin and, therefore, is independent of its crystallinity. Our study includes the comparison of different native cellulose specimens with (i) a completely disordered reference sample and (ii) a sample where the *intracrystalline* hydroxyl groups have been deuterated. Thus, we can state that the accessible regions are identical to disordered regions. These regions, which include the crystal surfaces, possess a common *dynamic* signature.

1. Introduction

Cellulose, the most abundant biopolymer, is a linear stereoregular homopolymer composed of anhydrous D-glucopyranose units that are connected by β-(1→4)-glycosidic linkages. Its degree of polymerization (DP) varies over a large range depending on the cellulose origin. Biosynthesized as the main structural material in cell walls of all higher plants (and also in some marine animals), cellulose occurs usually combined with lignin, other polysaccharides ("hemicellulose"), and proteins. The structure and organization of cellulose define the properties of the macroscopic material and are of equal importance for the chemical reactions taking place during industrial processing.[1] In addition, from structural properties, conclusions can be drawn on cellulose synthesis in plants. A systematic description of cellulose material comprises three hierarchical levels: (i) The *molecular* level describing the single molecule; (ii) the *supermolecular* level concerning the packing and aggregation of the molecules in crystals called *microfibrils* with diameters characteristic for a given species; and (iii) the *morphological* level, i.e., the arrangement of microfibrils and interstitial voids in relation to the cell wall.

On the molecular and supermolecular level the potential of cellulose to establish extended networks involving intra- and intermolecular hydrogen bonds is particularly important. The detailed structure of these networks is still subject to discussion and has led to several models (recently reviewed by O'Sullivan[2]). The intramolecular hydrogen bonds stiffen the chains along their axis while the intermolecular hydrogen bonds—assisted in their task by van der Waals interactions—are responsible for chain packing and aggregation.[3]

Concerning the morphology of native cellulose, the "classical" two-phase models[4−6] assuming crystalline and amorphous parts apparently have to be revised. Recent experimental results are rather in favor of a model for the plant cell wall where just the surface of isolated microfibrils is disordered: (i) By means of high-resolution, low-dose electron microscopy, a lattice imaging of cellulose microfibrils has been achieved.[7] (ii) Biosynthesis of cellulose microfibrils takes place in organized macromolecular structures (*terminal complexes*) in the plasma membrane,[8] which produce microfibrils of a specific size, but no isolated cellulose molecules.[9] (iii) Cross-polarization, magic-angle spinning (CP/MAS) ^{13}C NMR spectroscopy is able to discriminate between cellulose molecules inside and outside the crystals.[10] The percentage of crystalline cellulose found by NMR is relatively high. This result may be satisfactorily explained by disordered cellulose molecules on microfibril surfaces but not in extended, separate amorphous regions.[11,12]

However, the presence of disordered regions is a stringent consequence of other experimental findings: e.g., the tensile properties of cellulose fibers such as ramie or flax cannot be fully understood just on the basis of the elastic constants of purely crystalline cellulose.[13] The present work is aimed at contributing to the discussion on "amorphous" native cellulose. Concepts such as crystallinity and amorphicity are well-adapted to describe homogeneous states of matter. They are on the other hand rather ill-defined when it comes to treat dense composite materials like cellulose given that intermolecular correlations do not build up or die off abruptly at some fictitious interfaces. For microfibrils measuring only a few nanometers in diameter, we expect a smeared out interface to the surrounding

* To whom correspondence should be addressed (E-mail: mmueller@esrf.fr).
† Institut für Materialphysik der Universität Wien.
‡ European Synchrotron Radiation Facility.
§ Institut Laue-Langevin.
|| Hahn-Meitner-Institut.
⊥ University of Tokyo.

10.1021/ma991227l CCC: $19.00 © 2000 American Chemical Society
Published on Web 02/12/2000

disordered medium. This medium, on the other hand, cannot be termed amorphous in the strict sense, as it must retain some directionality from the microfibril environment.[14] The conceptual difficulties make the interpretation of diffraction experiments problematic and explain why numerical values for crystallinity extend over a wide range (±25%) in the literature depending on the experimental methods used.[2,6,12]

A by far better defined quantity than crystallinity or amorphicity is the *accessibility* of cellulose to various guest molecules, in particular water.[15] In this paper we will show that the accessible regions may unambiguously be identified with the disordered regions of a specimen, which show universal dynamical signatures.

Using the hydroxyl groups of the cellulose as a microscopic probe, we investigated the dynamic response of regions accessible to water, $\chi''_{ac}(\omega)$,by means of inelastic neutron scattering (INS). A low-energy neutron spectrum reflects the structure of matter with all its different kinds of atoms, bonds, and electronic states and is, therefore, sensitive to properties on a local length scale well-adapted to the problem. It is a well-known fact that disorder is particularly reflected in the low-frequency dynamics: cellulose is no exception to this general rule as was recently shown by INS.[16] $\chi''_{ac}(\omega)$ for the accessible regions is distinctly different from the one obtained for the crystal cores [$\chi''_{inac}(\omega)$] and may, therefore, constitute a signature of the disordered state. All these signatures turn out to be identical when comparing cellulose types of different crystallinity, indicating its universal character. This comparison includes a completely disordered *amorphous* reference sample underlining the universality further and in addition demonstrating the identity of $\chi''_{ac}(\omega)$ and $\chi''_{disorder}(\omega)$, where the latter denotes the response of the disordered regions.

The paper starts with a short description of the experimental technique of INS. We will then say some words on the selective deuteration technique, which allows us to experimentally discriminate the hydroxyl group dynamics inside and outside the crystalline cellulose microfibrils. Further experimental details on samples and instruments used will be given. Finally, the results obtained on cellulose samples of different origin and degree of crystallinity are discussed.

2. Experimental Techniques

2.1. Neutron Time-of-Flight Spectroscopy. Inelastic neutron scattering (INS) and in particular neutron time-of-flight spectroscopy enables us to measure the dynamic response of cellulose samples in the picosecond region where collective lattice vibrations take place. The scattering process is described by the double-differential cross section $d^2\sigma/d\Omega\, dt$, which gives the fraction of neutrons of incident wavevector $\mathbf{k}_i$ scattered into an element of solid angle $d\Omega$ during the time interval $[t, t + dt]$. It can be directly converted into $d^2\sigma/(d\mathbf{Q}\, d\hbar\omega)$ with $\mathbf{Q}$ and $\hbar\omega$ denoting the wave vector and energy transfer, respectively.[17]

The double-differential cross section is related to the generalized—i.e., neutron scattering power weighted—susceptibility, $\chi''(\mathbf{Q},\omega)$, via

$$\frac{d^2\sigma}{d\mathbf{Q}\, d\hbar\omega} \propto \{1 + n(\omega)\}\chi''(\mathbf{Q},\omega) \qquad (1)$$

$n(\omega)$ is the detailed balance factor $[1 - \exp(-\hbar\omega/k_B T)]^{-1}$. The generalized susceptibility is an intrinsic sample property that can be directly compared to predictions based on linear response theory.

Table 1. Scattering Powers p_i for the Nuclei Present in Cellulose

	C	O	H	D
c_i (%)	28.57	23.81	47.62	47.62
p_i (10^2 barn/amu)	13.2	6.3	3875.0	181.8

An intuitively more tangible quantity is the phonon density of states, $G(\omega)$. In the one-phonon incoherent approximation[18] it is obtained from the double-differential cross section via

$$\int_{\Theta_{min}}^{\Theta_{max}} d\Theta \sin\Theta \frac{d^2\sigma(2\Theta,\omega)}{d\Omega\, d\omega} \propto u(\omega)\sum_i \frac{c_i\sigma_i}{M_i}F_i(\omega) = G(\omega) \qquad (2)$$

with

$$u(\omega) = \frac{Q_{max}^4 - Q_{min}^4}{\hbar\omega[\exp(-\hbar\omega/k_B T) - 1]} \qquad (3)$$

σ_i/M_i is the scattering power of element i with concentration c_i. $F_i(\omega)$ is the partial density-of-states of element i.

For the relative comparisons on which the arguments in this paper will based, it turns out sufficient to deal directly with the angle-integrated time-of-flight spectra, knowing that these are related unambiguously to more physical quantities such as $\chi''(\mathbf{Q},\omega)$ or $G(\omega)$. The main advantage of this approach exists in the preservation of data statistics.

2.2. Accessibility and Scattering Contrast. Throughout this work we benefit from the neutron scattering contrast that exists between hydrogen and deuterium. The inelastic neutron spectrum of cellulose is dominated by the scattering from protons (see scattering powers in Table 1). Protons that are part of OH groups have the characteristic of being exchangeable by deuterium in the course of a D_2O wetting process if accessible to water. Difference spectra of a protonated sample and an identical one but with H in hydroxyl groups exchanged by D then reflect the dynamical response of exchanged OH groups on accessible cellulose molecules. The contrast can also be raised if the scattering of the inaccessible parts is reduced. This is accomplished by deuterating the hydroxyl groups inside the crystals, which is not possible under normal conditions due to an unperturbed hydrogen-bond network.[15] Deuteration inside the crystals is, however, possible using a relatively simple hydrothermal treatment technique[19] (see Section 3.1): All OH groups *inside* the crystalline parts can be deuterated without affecting the morphology of the crystals. In an analogous way as "normal" deuteration works, a re-exchange from OD to OH in the accessible parts is possible by using H_2O. In the following paragraphs, we denote such cellulose as "inversely" deuterated. A schematic picture of deuteration of cellulose with accessibility a ($0 \le a \le 1$) is shown in Figure 1. The degree of deuteration itself can be unambiguously determined from the neutron scattering experiment. It is established both via the elastic and/or inelastic incoherent signals. While the elastic signal offers better statistics, the interference effects due to coherence are, in our opinion, better dealt with in the inelastic part of the spectra: The coherent contribution to the elastically scattered intensity gives rise to pro-

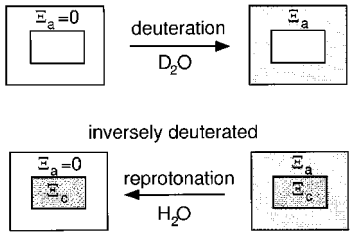

Figure 1. Scheme of cellulose deuteration with accessibility *a* for a "normal" sample (above) and an inversely deuterated sample (below). $\Xi_{a,c}$ denotes the degree of deuteration outside and inside the crystals, respectively. In both cases, crystal cores are unaffected by immersing the sample in D_2O or H_2O, i.e., inaccessible.

nounced Bragg reflections, whereas the influence of coherence on the energy-integrated inelastic signal is weaker. A good approximation is, therefore, the integration of the signal over a large angular range (incoherent approximation[18,20]).

It is possible to establish the link between INS intensities and water accessibility *a* into a more mathematical form. We label the accessible regions by their finite degree of deuteration Ξ_a. Note that Ξ_a is an integral quantity obtained by averaging the local level of deuteration $\xi_a(\mathbf{r})$ over the accessible regions. In the *homogeneous* deuteration case ξ_a is independent of $\mathbf{r}$ and therefore $\Xi_a = \xi_a$. The connection between the INS signal and the degree of deuteration is established via the average scattering power $\Sigma = \sum_i c_i\sigma_i/M_i$. c_i and σ_i stands for the concentration and bound scattering cross section of element *i*, respectively (for numerical values see Table 1). Written as a function of Ξ_a, we get the following for cellulose not deuterated in the crystalline parts:

$$\Sigma(a) = p_C + p_O + p_H + a\Xi_a(p_D - p_H) \qquad (4)$$

with $p_i \equiv c_i\sigma_i/M_i$. If we know

$$r(a) = \Sigma_{after}(a)/\Sigma_{before}(a) \qquad (5)$$

i.e., the ratio of the mean scattering power before and after H/D exchange, we are able to determine *a* with the help of eq 4 experimentally:[21]

$$a\Xi_a = (1 - r)\frac{p_C + p_O + p_H}{p_H - p_D} \approx 1.05(1 - r) \qquad (6)$$

Evidently, the factor of 20 between the scattering power of hydrogen and deuterium makes this contrast technique very powerful. Equation 6 shows what is already intuitively clear: the accessibility can only determined from the scattering contrast if Ξ_a is known and vice versa. The largest contrast corresponding to the minimum ratio $r_{min} \equiv 71.5\%$ is obtained for $a = 1$ and $\Xi_a = 30\%$, i.e., 100% accessible and H/D exchanged cellulose.

Equation 2 demonstrates that $r(a)$ can be obtained from energy and angle integrated INS signals

$$\int_{\omega_a}^{\omega_b} d(\omega) \int_{\Theta_{min}}^{\Theta_{max}} d\Theta \sin\Theta \frac{d^2\sigma(2\Theta,\omega)}{d\Omega\, d\omega} \qquad (7)$$

under the condition that deuteration does not change the partial densities of state $F_i(\omega)$. This is true to a very good approximation for the low-frequency region which dominates the INS signal as easily verified by varying the integration limit ω_b in eq 7. Deuteration influences the vibrational frequencies due to the change in mass when substituting deuterium for hydrogen. This influence is negligible for low-frequency modes, where the light hydrogen or deuterium atoms move in phase with the glucose residues.

3. Experimental Details

3.1. Sample Preparation. As shown in Table 2, we investigated four different *native* cellulose samples and artificially produced amorphous cellulose in order to vary the degree of cellulose accessibility. The purification of parenchymal cellulose from *sugar beet* pulp is described elsewhere.[22,23] This sample essentially consists of primary cell wall cellulose. The *tunicate* cellulose was extracted from the mantle of *Halocynthia roretzi*, a marine animal. It was deproteinized and bleached[24] and afterward hydrolyzed overnight in 50 wt % aqueous sulfuric acid at 40 °C in order to yield a suspension of tunicate cellulose microcrystals. From this suspension, a thin film of cellulose was prepared. The bleached *flax* fibers were combed and aligned in one direction, achieving a sample thickness of approximately 0.1 mm. *Cotton* linters were used without any further treatment. Flax and cotton were characterized in an X-ray diffraction experiment (laboratory source, $\lambda = 1.54$ Å).

For comparison, an artificially produced purely *amorphous* cellulose sample was investigated: A thin film of amorphous cellulose was cast from the melt of a 10% solution of cellulose (DP = 600) in *N*-methylmorpholine *N*-oxide, monohydrate (NMMO). The NMMO was exchanged with anhydrous methanol and dried under vacuum for 24 h at $T = 400$ K.[25] To characterize the amorphous cellulose, we measured the static structure factor $S(Q)$ at the high-flux neutron powder diffractometer D20 at Institut Laue-Langevin (ILL). As it is typical for amorphous substances, the diffraction pattern shows a broad structure factor maximum at $Q \approx 1.5$ Å^{-1} instead of Bragg peaks. A second amorphous sample, prepared by regeneration of cellulose from its solution in SO_2−diethylamine−dimethyl sulfoxide,[26] was investigated for comparison.

In the case of inverse deuteration, samples were inserted into glass ampules filled with 0.1 N NaOD/D_2O. The sealed ampules were kept at 210 °C for 30 min.[19] As recently shown,[19] the morphology of the crystals is unaffected by this process.

3.2. INS Experiments. All INS measurements were carried out using the cold neutron time-of-flight (TOF) spectrometer IN6 at ILL in Grenoble.[27] The wavelength of the incident neutrons was $\lambda = 4.12$ Å, corresponding to an energy resolution at the position of the elastic line of $\delta\Delta E \approx 200$ μeV (fwhm). The flat sample containers (see below) were mounted into a heating/cooling loop and positioned at an angle of 22° with respect to the incident neutron beam in order to avoid multiple scattering and strong absorption effects. Measuring times were between 3 and 6 h. Normalization, detector efficiency correction, and subtraction of the empty aluminum container contribution were carried out for every spectrum.

One experimental cycle involves measurement of both the protonated and the in situ deuterated sample. It, therefore, consists of the following steps: After carefully drying the sample at 350 K in a vacuum oven ($p \approx 10^{-2}$ mbar) it was inserted into a sieve-shaped aluminum container covering an area of ≈ 10 cm^2. Once mounted in the instrument, the position of the container was kept fixed for the whole experimental cycle. In the first stage of the experiment we measured the dry, fully protonated sample at a temperature $T = 310$ K. The sample was then in situ immersed for 20 min in heavy water for deuteration.[28] After drying—still in situ—in a vacuum ($p \approx 10^{-2}$ mbar) at 350 K for 90 min the now deuterated sample is measured at the same temperature as the previous protonated one ($T = 310$ K). Using this in situ process, we obtain extremely stable experimental conditions over one cycle in the sense that we always have exactly the same sample volumes (typical sample mass $m \approx 0.12$ g) illuminated by the neutron beam. Stability is essential for a data analysis involving difference spectra.

Table 2. Overview on Investigated Cellulose Samples[a]

	cotton linter	sugar beet parenchyma	tunicate	bleached flax fibers	amorphous cellulose
morphology	sheet	sheet	film	aligned fibers	(1) film (2) powder
thickness (mm)	0.1	0.1	0.1	0.1	0.2
deuteration technique	normal	inverse	normal, inverse	normal	

[a] Four native celluloses of different origin and degree of accessibility and artificially produced amorphous cellulose.

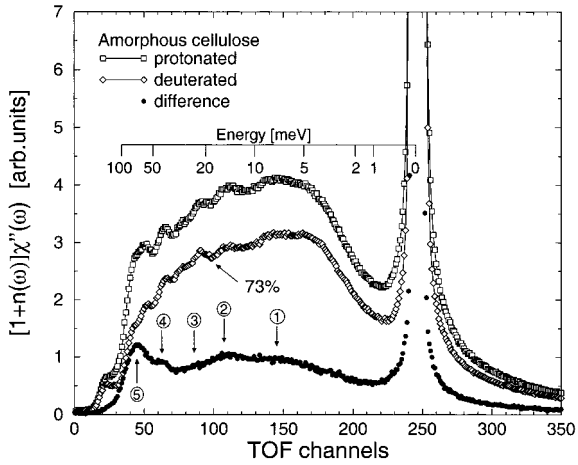

Figure 2. Effect on the low-energy dynamics by deuteration of polar (OH) groups in amorphous cellulose. The loss of intensity due to the diminution of the total scattering cross section can be estimated to 27%. The lower curve (filled circles) is the difference (OH − OD), which essentially reflects the dynamics of OH groups. The time-of-flight channels are directly correlated to the flight time by $t_F = 9.625(247 -$ channel no.) [μs]. Note that 1 meV = 8.006 cm^{-1}.

Table 3. Ratios *r* of Integrated Intensities for Amorphous Cellulose, Using Various Ranges of Integration

integration limits (meV)	r^a (%)	integration limits (meV)	r^a (%)
0.64−2.14	73.3	2.40−49.9	74.3
0.64−10.7	75.3	10.3−103.2	70.2
5.84−23.1	73.7	0.60−363	72.8

[a] An average $r = 73(2)\%$ is obtained.

In the case of an inversely deuterated sample, the fully deuterated sample was measured first, and the accessible parts were reprotonated in the same way as outlined above using H_2O (see Figure 1).

4. Results and Discussion

4.1. Low-Energy Dynamics of Amorphous Cellulose. The neutron spectra of amorphous cellulose are shown in Figure 2 (two upper curves). They are typical for a noncrystalline material with little structure but just a few broad peaks. Obviously, the in situ deuteration has a strong effect on the inelastically scattered intensity. The intensity loss upon deuteration may be analyzed quantitatively: integration of the inelastic intensities leads to a ratio of $r = 73(2)\%$ (Table 3) based on eqs 5 and 7.[29]

This *r* value is very close to the theoretical minimum $r_{min} \equiv 71.5\%$ and translates into an average chemical composition after deuteration equal to $C_6H_{7.15}D_{2.85}O_5$. Hence hydroxyl groups have been deuterated to $a = 95(7)\%$. The INS results, therefore, confirm that amorphous cellulose is indeed practically 100% accessible to water and that a nearly perfect exchange of OH groups is obtained in the accessible regions by simple wetting. This fact may be explained as follows: The amount of low-ordered regions is decisive for the hydrophilicity of a given cellulose material. The water content of completely disordered amorphous cellulose is about 47 wt % bound H_2O after wetting and subsequent removal of bulk water.[30] In this disordered material, all hydroxyl (OH) groups that are not completely saturated by hydrogen bonds—one could imagine a strong fluctuation of hydrogen bonds near defects, voids, or surfaces—can be affected by water molecules. Due to the penetration of water molecules, the sample swells and distances between cellulose molecules increase, additionally perturbing the hydrogen bonds between cellulose molecules. This process finally makes almost every hydroxyl group accessible to water molecules. Hence, swelling and washing of amorphous cellulose in D_2O will lead to a full exchange of OH by OD. This means an exchange of 30% of all hydrogens in the cellulose molecule. On removing heavy water by drying the sample, OD groups are preserved as long as the sample is protected against atmospheric humidity or other protonated polar solvents.

The difference spectrum between protonated and deuterated amorphous cellulose is also shown in Figure 2 (filled circles). Following the aforementioned, it essentially reflects the dynamical response of protons in OH groups.

At low-energy transfers the curve is smooth, featuring several broad bands marked by indices 1, 2, and 3 (at 7.7, 15, and 22 meV, respectively). In the higher energy range, two pronounced peaks are discernible at 40 and 70 meV (indices 4 and 5, respectively). Following the most recent normal mode calculations on cellulose,[31] we can assign excitations 4 and 5 to bending modes of the skeletal pyranose ring. Peaks 2 and 3 are visible in the difference spectrum because they involve stretching modes of the intramolecular hydrogen bonds,[31] thus, the dynamics of hydroxyl groups. No assignment can be made for the lattice mode of excitation 1 as the calculation[31] was carried out for the origin of the Brillouin zone, i.e., $Q = 0$, which is not sufficient to explain low-energy neutron spectra. As amorphous cellulose has the tendency to recrystallize in water, we cross-checked the experiment with the second amorphous sample prepared differently, which was shown to be stable in aqueous media.[26,32] The resulting difference INS spectrum is of the same shape.

In order for the difference spectra to constitute *fingerprints* of accessible regions of cellulose, two conditions must be fulfilled: (i) The difference spectrum has to be an intrinsic property of amorphous cellulose; it should, for example, not be contaminated by water contributions. (ii) The difference spectrum has to be specific to the accessible parts, i.e., it must be distinct from the OH response of inaccessible regions.

As it is essential for the arguments presented, we will now briefly demonstrate the validity of both conditions.

(i) A main characteristic of adsorbed water is the strong so-called quasielastic scattering around the elastic line due to the rotational and translational diffusion dynamics of water on the picosecond time scale.[30] It is not observed in the difference spectra (see Figure 2). Concerning the inelastic region, neither the

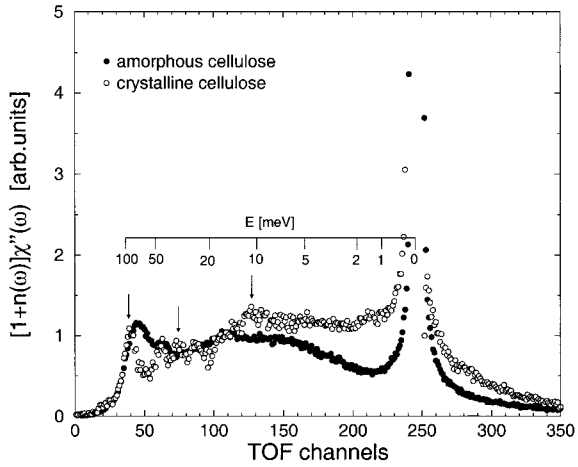

Figure 3. Comparison of neutron time-of-flight difference spectra of amorphous and crystalline cellulose. Please note that the "amorphous" spectrum is identical to that in Figure 2.

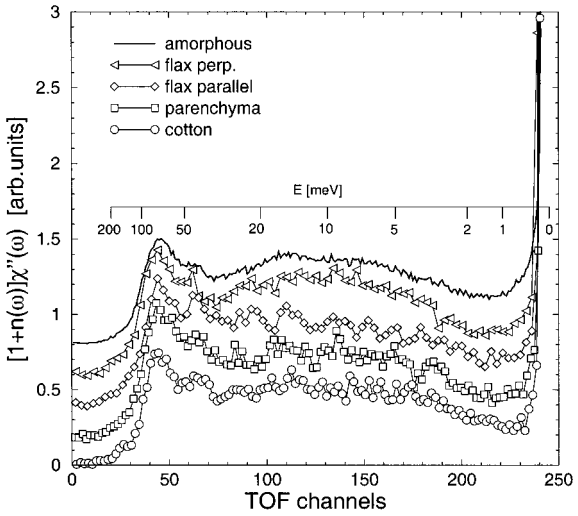

Figure 4. Comparison of difference spectra of different types of cellulose. The spectra are obtained in the same way as those in Figure 2. "Parallel" means flax fibers that are aligned in the scattering plane, "perpendicular" fibers oriented perpendicularly to it. Curves are shifted vertically by 0.2.

typical 7 meV phonon peak, found both in crystalline and amorphous ice forms,[33] nor the water librations above 90 meV are observed in the difference spectra. Thus, the moisture content is very low in both the protonated and deuterated samples.

(ii) To compare the dynamics of OH groups of accessible regions to those of inaccessible regions, we made use of the intracrystalline, i.e., *inversely* deuterated tunicate cellulose, sample. Tunicate cellulose is particularly suited for our purpose as the microcrystals have a relatively large cross section of 150 × 150 Å^2.[24] We determined the difference spectrum of a tunicate sample, which was completely protonated inside the crystals but had surface OH groups deuterated, and a fully OH/OD exchanged sample.[34] Figure 3 shows the comparison of the "amorphous" (same spectrum as in Figure 2) with this "crystalline" difference spectrum. Essentially, the dynamic response of inaccessible hydroxyl groups consists of several sharp excitations, in strong contrast to the much less structured spectrum of the accessible hydroxyl groups. Some particularly strong differences are indicated by arrows. In particular, the ring bending modes[31] are considerably harder, i.e., they are of higher frequency, in crystalline cellulose (centered at 90 meV), indicating a much higher chain flexibility in the accessible parts. An additional excitation band is observed at 33 meV that does not occur in the amorphous difference spectrum. This mode was assigned to stretching of an intramolecular hydrogen bond, which is possibly disrupted in disordered cellulose.[31]

In conclusion, the difference spectrum in Figure 2 can well be regarded a fingerprint of hydroxyl group low-energy dynamics of disordered or accessible cellulose. We denote this characteristic dynamic response as $\chi''_{ac}(\omega)$ and the corresponding signature of crystalline, i.e., inaccessible cellulose (see discussion under ii above), with $\chi''_{inac}(\omega)$.

4.2. Low-Energy Dynamics of Disordered Parts in Native Cellulose. The low-energy dynamics of accessible OH groups in natural cellulose—$\omega^{-1}\chi''_{ac}$—is shown in Figure 4 as a function of the cellulose origin. Even without quantitative analysis it is evident that the samples with no preferred orientation (almost powder texture), namely cotton, sugar beet pulp, and amorphous cellulose, all show identical spectra within the experimental uncertainties; as amorphous cellulose is fully accessible to water it constitutes the ideal reference to which the accessible regions of the native samples should be compared. In particular all three spectra exhibit equally pronounced excitations at $\Delta E = 70$ and 40 meV. The dynamical OH response of the accessible regions in native cellulose, therefore, seems to be universal.

Distinct deviations from this universal behavior occur in the spectra of oriented flax fibers. As the INS experiment determines the projection of the vibrational amplitudes onto the wavevector transfer **Q**, this directional dependence reflects the anisotropic nature of the disordered regions within the fibers. There is also evidence from X-ray scattering for this finding.[14] The disordered regions, therefore, cannot be termed amorphous in the classical sense. They rather constitute the interface between microfibrils and as such possess an intrinsic directionality induced by the morphology of native cellulose.

There is an excess of intensity at low frequencies for fibers aligned perpendicularly to the scattering plane. This excess indicates that the OH groups vibrate dominantly within the equatorial plane of the fibers. That the *transverse* modes are found at lower frequency if compared to the ones with polarization vector along the fiber is best demonstrated by looking at the generalized densities of states of the fully protonated sample (Figure 5). The increase in the low-frequency regime is found to be steeper for flax aligned perpendicular to the scattering plane than for flax aligned parallel, corresponding to a shift of frequencies to lower energies. In other words, a flax fiber is stiffer along the fiber axis than perpendicular to it. This is not surprising as the equatorial plane motions are governed by the rather weak hydrogen bonds connecting the chains in the lateral direction and van der Waals forces between these sheets of chains, while motions along the fiber axis are dominated by strong covalent bonds.

4.3. Accessibility and Morphology. To put the observed universality of the dynamic response into perspective, we have a closer look at cellulose morphology. In particular, we will discuss the question of how the volume of accessible regions compares to the one of crystalline surface layers. If we assume that Ξ_a in the

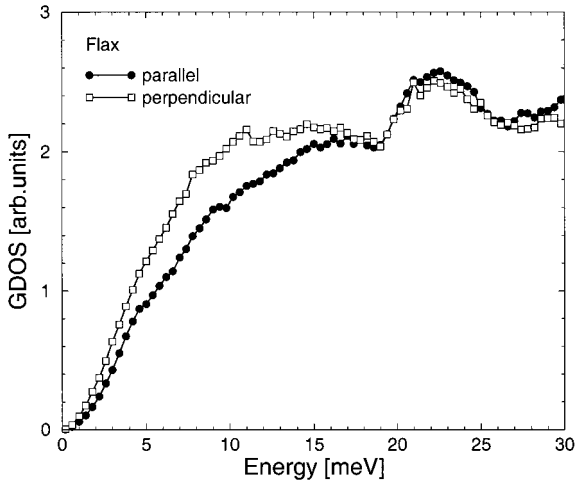

Figure 5. Comparison of generalized densities of states of flax fibers oriented in a parallel and perpendicular way with respect to the scattering plane.

native samples is identical to Ξ_a of amorphous cellulose, i.e., $\Xi_a = 30\%$, we may determine the accessibilities a as in section 2.2. Numerical values of r_{INS} and a_{INS} are given in the first two columns of Table 4. The error of r is on the order of 2% (see Table 3), leading consequently to an error in a of about 7%. In the case of highly crystalline tunicate cellulose, the effect of deuteration is almost negligible, thus, too low for reliably estimating the accessibility. For the other cellulose specimens, accessibility ranges from 41% (cotton) to 56% (vertical flax fibers).

As we will demonstrate in the following, the measured accessibilities can be set into relation with microfibril geometry. We take data on crystal cross sections from recent works on identical samples of parenchymal cellulose[23] and tunicate cellulose.[24] The respective values for cotton and flax were obtained in laboratory X-ray diffraction experiments (see section 3.1). In general, it appears to be less problematic to extract crystal sizes from diffraction results than from small-angle scattering experiments, as discussed recently[35] for the exemplary case of flax. Almost rectangular microfibril cross sections are assumed, with the edges of the equatorial plane parallel to $(1\bar{1}0)$ and (110) and one diagonal parallel to (200) (notation of Sarko and Muggli[36]). Using the lattice spacings $d_{1\bar{1}0} = 6.00$ Å, $d_{110} = 5.35$ Å,[36] the number of cellulose chains in the crystal and on its surface are easily calculated and given in Table 4.

Native cellulose is produced by living organisms as organized microfibrils. It is, therefore, reasonable to assume that the interface between two microfibrils comprises two surface layers. As about half of the hydroxyl groups on the surface chains point toward the interior of the crystals, the surface accessibility, a_{surf}, should be given to a very good approximation by half of the numerical ratio of surface to total chains. The accessibility measured by deuterium exchange may only be smaller than a_{surf} if some OH groups of the surface chains are too strongly bound to be exchangeable.

Apart from tunicate and parenchymal cellulose, the accessibilities derived from INS (a_{INS}) are about a factor 2 larger than a_{surf}. We, therefore, deal with additional disordered molecules outside the crystalline domains. A good candidate for such disorder, compatible with all our experimental results, is a single interface layer between neighboring crystals. In the special case of flax fibers, we measured two difference spectra, one with the fiber axis of flax perpendicular to the scattering plane, the other one where the fiber axis is in this plane. Thus, in the first case only scattering in lateral direction of the fiber is detected, while in the other case the scattering signal is a combination of scattering perpendicular and along the fiber axis (in fact, the latter contribution dominates).[16] In deriving eq 2, we averaged over all polarization vectors in space. As the calculation of accessibility according to eq 6 is only valid for a powder, deviations between effective accessibilities of flax fibers aligned parallel or perpendicular to the scattering plane have to be expected.

5. Conclusions

We have demonstrated that the low-frequency dynamical response as determined by INS is a well-suited quantity to characterize composite polymeric materials such as cellulose. It turns out that the restoring forces, which are encountered by OH groups when averaging over the accessible parts of native cellulose, are completely different from those obtained on inaccessible parts. The INS spectra of the disordered cellulose molecules have the typical shape of those of amorphous materials: The accessible regions, therefore, correspond to disordered cellulose chains, the inaccessible ones to those inside crystals. The disordered molecules, however, retain a preferential orientation parallel to the chains in the microfibrils. Taking into account the accessibility of the samples under investigation, we conclude that the major part of disordered chains is surface molecules of the microfibrils. Despite the preferential orientation, the surface chains are sufficiently disordered to be termed "amorphous". With respect to X-ray diffraction and small-angle scattering results,[14,35] these may be explained on the basis of surface disorder; thus, there is no need to assume extended disordered regions between or within the microfibrils. We propose nonsurface disordered cellulose chains to constitute a sort of interface layer between neighboring microfibrils,

Table 4. Measured Ratios of Integrated Intensities (r_{INS}) and Accessibilities (a_{INS}) for Different Kinds of Cellulose, Given in Ascending Order of a_{INS}[a]

cellulose type	r_{INS} (%)	a_{INS} (%)	A (Å^2)	n° of molecules		a_{surf} (%)
				surface	integral	
tunicate	98(2)	7(7)	150 × 150[24]	102	700	7
parenchyma	86(2)	40(7)	30 × 30[23]	17	28	30
cotton	88(2)	41(7)	49 × 66 (this work)	37	101	18
flax par	87(2)	46(7)	41 × 44 (this work)	26	56	23
flax perp	84(2)	56(7)	41 × 44 (this work)	26	56	23

[a] The sample of parenchymal cellulose was OH/OD exchanged inside crystalline parts. For the estimation of surface accessibility, a_{surf}, a rectangular cross section A [edges parallel to $(1\bar{1}0)$ and (110) planes, respectively] of the cellulose microfibrils was assumed. Half of all hydroxyl groups in surface molecules should be accessible to water. The number of molecules was calculated using $d_{1\bar{1}0} = 6.00$ Å, $d_{110} = 5.35$ Å.

since this agrees very well with the accessibilities measured.

When performing a powder average (this was in fact inherent to all of our samples except the oriented flax fibers), the dynamic response of disordered native cellulose is indistinguishable from that of artificial amorphous cellulose. The disordered regions apparently are of universal nature in terms of their INS spectra. As these are very sensitive to the *local* properties of molecules, the accessible cellulose chains are very similar in terms of the hydrogen-bond network holding them together.

Acknowledgment. The authors wish to thank H. Chanzy for providing the native cellulose samples and critical reading of the manuscript, L. Heux for preparing the films of amorphous cellulose, A. Isogai for supplying amorphous cellulose, H. Requardt for help with the X-ray laboratory experiment (CNRS Cristallographie, Grenoble), and T. Hansen for experimental support in the diffraction experiment on D20 (ILL).

References and Notes

(1) Klemm, D.; Philipp, B.; Heinze, T. *Comprehensive Cellulose Chemistry*; John Wiley & Sons: New York, 1998.
(2) O'Sullivan, A. C. *Cellulose* **1997**, *4*, 173−207.
(3) Crystals in regenerated or mercerized cellulose (cellulose II) form a hydrogen network in both crystallographic directions perpendicular to the polymer chain.
(4) Nägeli, C. *Mizellartheorie* (reprinted); Oswalds Klassiker No. 227, A. Frey: Leipzig, 1928.
(5) Krässig, H. *Textilveredelung* **1969**, *4*, 26.
(6) Krässig, H. A. *Cellulose: Structure, Accessibility and Reactivity*; Polymer Monographs 11; Gordon and Breach Science Publishers: Yverdon, 1993.
(7) Sugiyama, J.; Harada, H.; Fujiyoshi, Y.; Uyeda, N. *Mokuzai Gakkaishi* **1984**, *30*, 98−99.
(8) Brown, R. M., Jr.; Saxena, I. M.; Kudlicka, K. *Trends Plant Sci.* **1996**, *1*, 149−156.
(9) Cousins, S. K.; Brown, R. M., Jr. *Polymer* **1995**, *36*, 3885−3888.
(10) Earl, W. L.; VanderHart, D. L. *Macromolecules* **1981**, *14*, 570−574.
(11) Smith, B. G.; Harris, P. J.; Melton, L. D.; Newman, R. H. *Plant Cell Physiol.* **1998**, *39*, 711−720.
(12) Heux, L.; Dinand, E.; Vignon, M. R. *Carbohydr. Polym.* **1999**, *40*, 115−124.
(13) Ishikawa, A.; Okano, T.; Sugiyama, J. *Polymer* **1997**, *38*, 463−468.
(14) Müller, M.; Czihak, C.; Burghammer, M.; Riekel, C. *J. Appl. Crystallogr.* In press.
(15) Ioelovitch, M.; Gordeev, M. *Acta Polym.* **1994**, *45*, 121−123.
(16) Müller, M.; Vogl, G.; Schober, H.; Chanzy, H.; Heux, L. In *Biological Macromolecular Dynamics*; Cusack, S., Büttner, H., Ferrand, M., Langan, P., Timmins, P., Eds.; Adenine Press: Schenectady, NY, 1997; pp 99−103.
(17) Bée, M. In *Quasielastic Neutron Scattering*; Adam Hilger: Bristol, PA, 1988.
(18) Taraskin, S. N.; Elliott, S. R. *Phys. Rev. B* **1997**, *55*, 117−123.
(19) Nishiyama, Y.; Isogai, A.; Okano, T.; Müller, M.; Chanzy, H. *Macromolecules* **1999**, *32*, 2078−2081.
(20) Schober, H.; Tölle, A.; Renker, B.; Heid, R,; Gompf, R. *Phys. Rev. B* **1997**, *56*, 5937−5950.
(21) In the case of inversely deuterated samples eqs 4 and 6 have to be modified: $\Sigma(a) = p_C + p_O + p_H + (p_D - p_H)[\Xi_c(1 - a) + a\Xi_a]$ and $a \approx 2768.5(1 - r)/[3693.2\Xi_a - 1108(1 - r)]$, assuming that the deuteration inside crystalline regions reaches the maximum value of $\Xi_c = 30\%$.
(22) Dinand, E.; Chanzy, H.; Vignon, M. R. *Cellulose* **1996**, *3*, 183−188.
(23) Dinand, E.; Chanzy, H.; Vignon, M. R. *Food Hydrocolloids* **1999**, *13*, 275−283.
(24) Favier, V.; Chanzy, H.; Cavaillé, J. Y. *Macromolecules* **1995**, *28*, 6365−6367.
(25) Montès, H.; Mazeau, K.; Cavaillé, J. Y. *Macromolecules* **1997**, *30*, 6977−6984.
(26) Isogai, A.; Atalla, A. H. *J. Polym. Sci. A* **1991**, *29*, 113−119.
(27) Institut Laue-Langevin Web site is http://www.ill.fr/Yellow-Book/IN6/ .
(28) The time needed for complete hydrogen−deuterium exchange (20 min) was checked in advance by infrared spectroscopy. The changes to the IR spectra in the region of OH and OD stretching modes reach equilibrium conditions after 10−15 min of immersion in D_2O.
(29) In Table 3 the ratios for different choices of the integration limits are listed. The higher the energy transfer of the lower integration limit, the more the ratio deviates: at high energies, the amplitudes of excitations are more and more affected by deuteration, and they are shifted in frequency. The error of *r* given in the text is estimated from the ratio's deviations in Table 3.
(30) Czihak, C.; Müller, M.; Schober, H.; Heux, L.; Vogl, G. *Physica B* **1999**, *266*, 87−91.
(31) Tashiro, K.; Kobayashi, M. *Polymer* **1991**, *32*, 1516−1526.
(32) This stability against recrystallisation is very probably responsable for the lower accessibility of $a = 80(7)\%$; i.e., there are inaccessible disordered regions present in this type of amorphous cellulose.
(33) Schober, H.; Koza, M.; Tölle, A.; Fujara, F.; Angell, C. A.; Böhmer R. *Physica B* **1998**, *241−243*, 897−902.
(34) The deuteration of the fully exchanged sample could not be carried out in situ. To scale the two spectra correctly when taking the difference, a completely OH/OD exchangeable crystalline core was assumed; however, the surface was not taken into account. The possible error is estimated to be small as the accessibility is very low (see Table 4). Therefore, artifacts are unlikely to appear, especially when comparing to "amorphous" and "crystalline" raw time-of-flight spectra.[16]
(35) Müller, M.; Czihak, C.; Vogl, G.; Fratzl, P.; Schober, H.; Riekel, C. *Macromolecules* **1998**, *31*, 3953−3957.
(36) Sarko, A.; Muggli, M. *Macromolecules* **1974**, *7*, 486−494.

MA991227L